

We-11-09

## Multisource Full Waveform Inversion of Marine Streamer Data with Frequency Selection

Y. Huang (KAUST) & G.T. Schuster\* (KAUST)

### SUMMARY

---

Multisource migration with frequency selection is now extended to multisource full waveform inversion (FWI) of supergathers for marine streamer data. There are three advantages of this approach compared to conventional FWI for marine streamer data.

1. The multisource FWI method with frequency selection is computationally more efficient than conventional FWI.
2. A supergather requires more than an order of magnitude less storage than the original data.
3. Frequency selection overcomes the acquisition mismatch between the observed data and the simulated multisource supergathers for marine data. This mismatch problem has prevented the efficient application of FWI to marine geometries in the space-time domain.

Preliminary result of applying multisource FWI with frequency selection to a synthetic marine data set suggests it is at least four times more efficient than standard FWI.

## Introduction

Multisource migration (Morton and Ober, 1998; Romero et al., 2000), least squares migration (LSM), and waveform inversion (Krebs et al., 2009; Virieux and Operto, 2009; Dai and Schuster, 2009; Tang, 2009) of phase-encoded supergathers were developed to significantly reduce the cost of migration and inversion. The key idea is to blend  $N$  encoded shot gathers into an  $N$ -shot supergather, and iteratively migrate encoded supergathers or, in the case of LSM or FWI, encoded supergather residuals. A representative formula for iteratively estimating the model parameter  $s_i$  in the  $i$ th cell is given by the steepest descent formula

$$s_i^{k+1} = s_i^k - \alpha \frac{\partial \varepsilon}{\partial s_i}, \quad (1)$$

where  $s_i$  can represent either the reflectivity or the slowness in the  $i$ th cell,  $\alpha$  is the step length, and  $\varepsilon$  is the misfit function<sup>1</sup> that is encoded after each iteration with a different encoding function. The benefit of this approach is that wave equation migration of each supergather costs about the same as the migration of a standard shot gather. If the number of iterations is fewer than  $N$ , then the computational cost of phase-encoded multisource imaging can be much less costly than separately migrating each of the  $N$  shot gathers (Schuster et al., 2011).

The problem with the above approach is that it is efficiently suited for land data where the receiver spread is fixed for each shot, but not for marine data with a receiver array that moves with each shot. As an illustration, Figure 1(a1) shows two shot gathers to be blended, where one shot is at the red source and the other is at the dark blue source; this 2-shot supergather will be denoted as  $\mathbf{d}^{obs.}$ . Typical of marine surveys, the receiver array is at a different offset for either source so that only certain receivers are *selectively* listening for the red shot but not for the dark blue shot at the non-overlapping receiver positions. In comparison, the predicted 2-shot supergather  $\mathbf{d}^{pred.}$  generated by a finite-difference<sup>2</sup> solution of the wave equation does not *discriminate* and generates traces at every receiver, as shown in Figure 1(a2). Hence, there will be discrepancies between the predicted and observed traces at the non-overlapping receiver positions (indicated by the dashed ovals in Figure 1). We will denote this problem in Multisource FWI (MFWI) as the *aperture mismatch* problem, where the observed supergather is for a blended marine survey while the predicted supergather is for a blended land survey.

The aperture mismatch will lead to a non-zero misfit function  $\varepsilon = \frac{1}{2} \|\mathbf{d}^{pred.} - \mathbf{d}^{obs.}\|^2$  even if the exact velocity model is used for prediction. The remedy to this mismatch is to use an encoding function in the multisource finite-difference modeling that only activates specified receivers for any one shot. This orthogonal encoding function strategy was developed by Huang and Schuster (2012) for wave equation migration, and will now be tested for FWI.

The first part of the paper provides the theory for multisource FWI with frequency selection, and is followed by results from tests with synthetic data. Preliminary tests show a speedup of  $4\times$  compared to conventional FWI. The last part presents a summary.

## Theory

The formula for multisource FWI is given in equation 1, where the velocity model is updated at each iteration and  $s_i$  represents the slowness model in each cell. The frequency selection encoding scheme is described in Huang and Schuster (2012), and summarized by the following steps.

1. Figure 1(a) illustrates the problem, and the first step is to assign a non-overlapping frequency

<sup>1</sup>The misfit function  $\varepsilon = \frac{1}{2} \|\mathbf{d}^{obs.} - \mathbf{d}^{ref.}\|^2$  relates to the  $L_2$  norm of the encoded difference between the predicted and observed supergathers.

<sup>2</sup>A finite-difference simulation of two *simultaneous* sources (a red source and a dark blue source) will compute traces everywhere on the surface that are a superposition of the wavefields from both sources.

spectrum to each of the sources. In Figure 1(b), the cyan (red) source is bandlimited around 20 Hz (10 Hz) during the multisource simulation and the supergather is computed.

2. In Figure 1(c), a bandpass filter is applied to decode the (b) supergather so that the cyan traces can be separated from the red traces. An appropriate muting of the traces at specified receivers for each shot is applied.
3. In Figure 1(d), the decoded and muted traces are blended together to give the bandlimited marine supergather. This procedure is iterated in equation 1, except that a unique non-overlapping frequency is assigned to each source. For a sufficient number of iterations, the full bandwidth of the data is employed at each source.

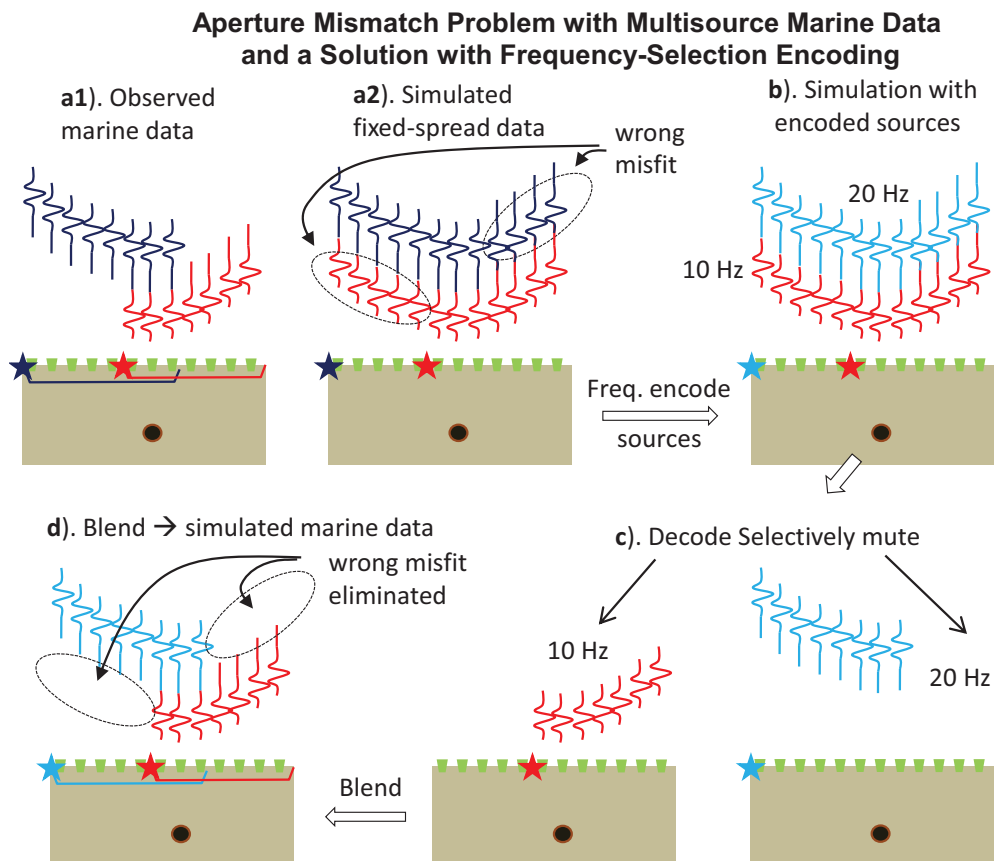


**Figure 1** The solution to the acquisition misfit problem illustrated in panels (a1) and (a2) on a single scatterer model, is given by the following steps: (b) the cyan (red) source is bandlimited around 20 Hz (10 Hz) during the multisource simulation; (c) a bandpass filter is applied to decode these bandpass filtered traces so that the cyan traces can be separated from the red ones. Muting of the specified traces for a marine geometry is applied. (d) The decoded and muted traces are blended together to give the bandlimited marine supergather. Now, there is no aperture mismatch between the simulated and observed supergathers, except that the frequency channels of the former are a subset of those of the latter.

## Numerical Results

We test the MFWI with frequency selection on SEG/EAGE salt model with a marine geometry; the model is decimated by a factor of  $3 \times 3$  for less overall computational time, as shown in Figure 2(b). The source wavelet is a Ricker wavelet peaked at 8 Hz; there are 60 shot gathers evenly distributed across the top of the model, with the shot spacing of 82.3 m; the receiver spacing is 27.4 m, and the line length is 2.3 km.

The FWI method uses a preconditioned conjugate gradient method, where the acoustic forward and backward solvers are a  $O(2,8)$  finite-difference solution to the 2D space-time wave equation of constant density. The source wavelet for the proposed frequency selection method is a pure cosine wave, also employed in Nihei and Li (2007) and Sirgue et al. (2008), at a selected frequency.<sup>3</sup>

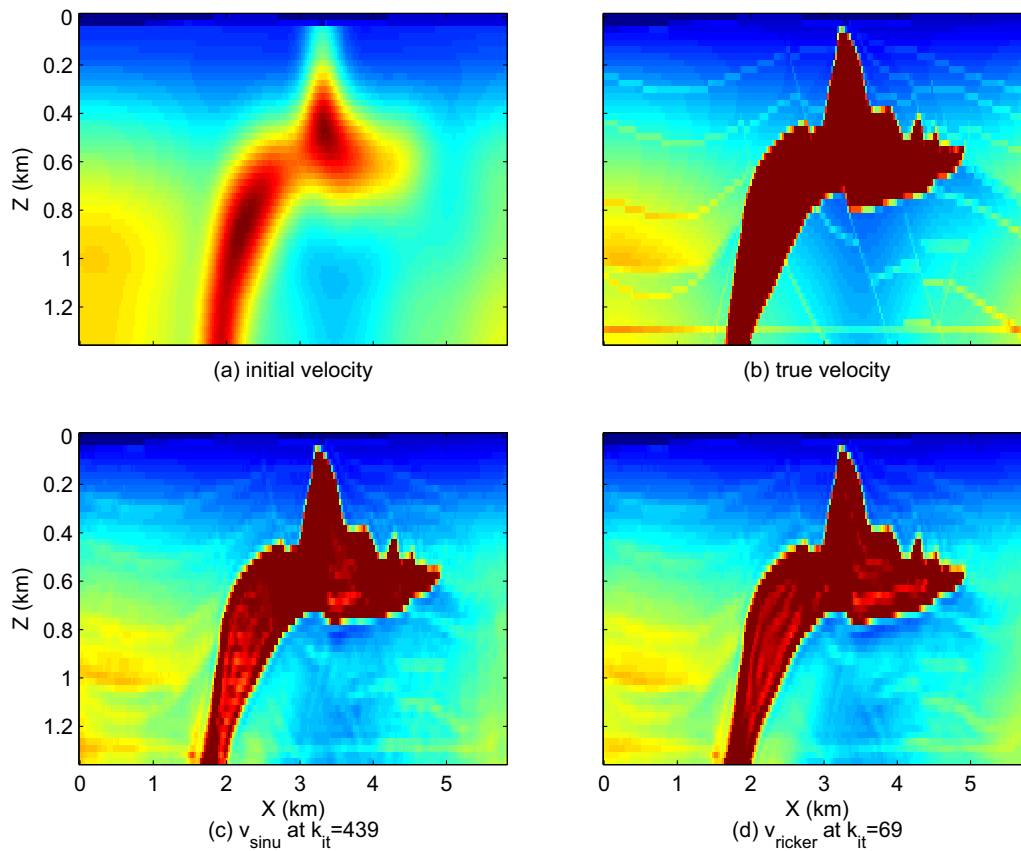


**Figure 2** (a) The initial velocity, (b) the true velocity, (c) the result of the proposed FWI at 439th iteration, and (d) the result of standard FWI at 69th iteration.

The starting model is shown in Figure 2(a), and the standard FWI tomogram after 69 iterations is shown in Figure 2(d). This result and the associated CPU time will serve as the standard metrics by which the MFWI algorithm will be measured.

The MFWI scheme with the frequency selection strategy produces the tomogram shown in Figure 2(c). This result required 439 iterations to achieve the same accuracy as the Figure 2(d) result in 69 iterations. This amounts to a factor of  $439/69 = 6.362$ . The convergence curves shown in Figure 3 are plotted in the way that the x-axes for the red dashed curves have been deliberately shrunk by 6.362. With this adjustment, the two convergence curves of velocity error in Figure 3(b) almost coincide with each other. Taking into account of this factor, among others such as the overhead of increased runtime per finite-difference run, as mentioned in footnote 3, the speedup over the conventional FWI scheme is estimated to be about 4. This compares to the  $8\times$  speedup reported by Huang and Schuster (2012) for RTM. One reason for this discrepancy is that the implementation in time domain sees a  $2\times$  overhead in order to reduce the effect of transients<sup>4</sup>. Better encoding and optimization schemes, which are topics for future research, may be able to relax this requirement. At present, the early results do suggest the possibility of a speedup with MFWI with frequency selection.

<sup>3</sup>To reduce the effect of transients in this wavelet, the simulation run time is doubled and the later half of the generated data, presumably in steady state, is retained for succeeding stages of FWI.

<sup>4</sup>Transient brings about bleeding—and therefore crosstalk—in the frequency domain.

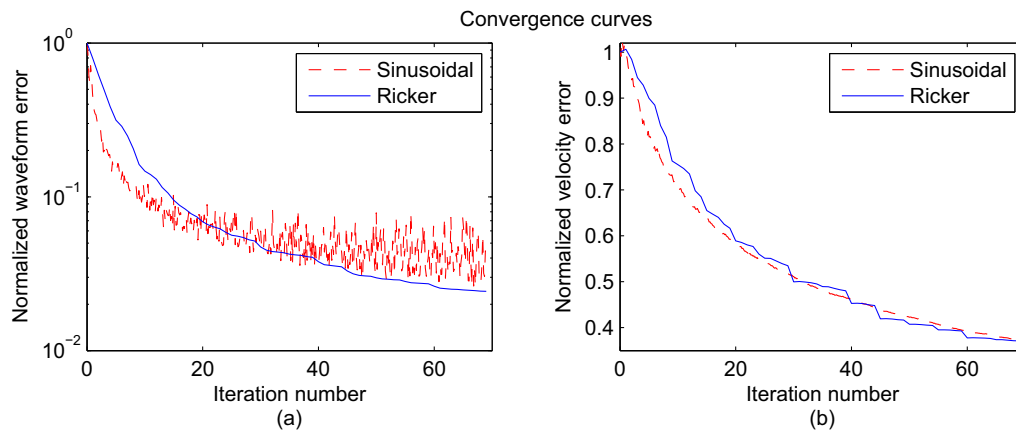


**Figure 3** Normalized error of waveform (a) and velocity (b) as functions of iteration number, for the proposed method (denoted by ‘Sinusoidal’) and the standard FWI (denoted by ‘Ricker’). Note that the iteration numbers for the red dashed curves are actually 6.362 times those in display. See text for details.

## Conclusions

Multisource full waveform inversion of supergathers for marine data is treated with frequency selection. The key enabling property of frequency selection is that it eliminates the crosstalk among sources, thus overcoming the aperture mismatch of marine multisource inversion. This method is now extended to implementation in the finite-difference time-domain from previous implementation in phase shift migration. Tests on FWI of synthetic marine data set suggests a 4× speedup is achieved.

## Acknowledgements

We wish to thank the sponsors of the Center for Subsurface Imaging and Fluid Modeling (CSIM) at KAUST for their support.

## References

- Dai, W. and Schuster, G.T. [2009] Least-squares migration of simultaneous sources data with a deblurring filter. *SEG Technical Program Expanded Abstracts*, **28**(1), 2990–2994, doi:10.1190/1.3255474.
- Huang, Y. and Schuster, G. [2012] Multisource least-squares migration of marine streamer and land data with frequency-division encoding. *Geophysical Prospecting*, **60**, 663–680.
- Krebs, J.R. et al. [2009] Fast full-wavefield seismic inversion using encoded sources. *Geophysics*, **74**(6), WCC177–WCC188, doi:10.1190/1.3230502.
- Morton, S.A. and Ober, C.C. [1998] Faster shot-record migrations using phase encoding. *68th Ann. Internat. Mtg. Soc. of Expl. Geophys.*, 1131–1134.
- Nihei, K. and Li, X. [2007] Frequency response modelling of seismic waves using finite difference time domain with phase sensitive detection (td-psd). *Geophysical Journal International*, **169**(3), 1069–1078.
- Romero, L.A., Ghiglia, D.C., Ober, C.C. and Morton, S.A. [2000] Phase encoding of shot records in prestack migration. *Geophysics*, **65**(2), 426–436, doi:10.1190/1.1444737.
- Schuster, G.T., Wang, X., Huang, Y., Dai, W. and Boonyasriwat, C. [2011] Theory of multisource crosstalk reduction by phase-encoded statics. *Geophysical Journal International*, **184**(3), 1289–1303.
- Sirgue, L., Etgen, J. and Albertin, U. [2008] 3d frequency domain waveform inversion using time domain finite difference methods. *Proceedings of the 70th EAGE Conference and Exhibition, Rome, Italy*, vol. 22.
- Tang, Y. [2009] Target-oriented wave-equation least-squares migration/inversion with phase-encoded hessian. *Geophysics*, **74**(6), WCA95–WCA107, doi:10.1190/1.3204768.
- Virieux, J. and Operto, S. [2009] An overview of full-waveform inversion in exploration geophysics. *Geophysics*, **74**(6), WCC1.